





Article

Effect of Additivized Biodiesel Blends on Diesel Engine Performance, Emission, Tribological Characteristics, and Lubricant Tribology

M. A. Mujtaba ^{1,2,*}, H. H. Masjuki ^{1,3}, M. A. Kalam ^{1,*} , Fahad Noor ², Muhammad Farooq ² , Hwai Chyuan Ong ⁴, M. Gul ^{1,5}, Manzoore Elahi M. Soudagar ¹ , Shahid Bashir ⁶, I. M. Rizwanul Fattah ^{4,*}  and L. Razzaq ²

¹ Department of Mechanical Engineering, Center for Energy Science, University of Malaya, Kuala Lumpur 50603, Malaysia; masjuki@um.edu.my (H.H.M.); mustabshirha@bzu.edu.pk (M.G.); manzoor@siswa.um.edu.my (M.E.M.S.)

² Department of Mechanical, Mechatronics and Manufacturing Engineering (New Campus), University of Engineering and Technology Lahore, Lahore 54000, Pakistan; f.noor@uet.edu.pk (F.N.); engr.farooq@uet.edu.pk (M.F.); luqmanrazzaq@uet.edu.pk (L.R.)

³ Department of Mechanical Engineering, Faculty of Engineering, The International Islamic University Malaysia, Kuala Lumpur 50728, Malaysia

⁴ School of Information, Systems and Modelling, Faculty of Engineering and IT, University of Technology Sydney, Ultimo, New South Wales 2007, Australia; HwaiChyuan.Ong@uts.edu.au

⁵ Department of Mechanical Engineering, Faculty of Engineering and Technology, Bahauddin Zakariya University, Multan 60000, Pakistan

⁶ Department of Physics, Center of Ionics, Faculty of Science University of Malaya Malaysia, University of Malaya, Kuala Lumpur 50603, Malaysia; shahidbashirbaig@um.edu.my

* Correspondence: m.mujtaba@uet.edu.pk (M.A.M.); kalam@um.edu.my (M.A.K.); rizwanul.buet@gmail.com or IslamMdRizwanul.Fattah@uts.edu.au (I.M.R.F.)

Received: 5 June 2020; Accepted: 26 June 2020; Published: 1 July 2020



Abstract: This research work focuses on investigating the lubricity and analyzing the engine characteristics of diesel–biodiesel blends with fuel additives (titanium dioxide (TiO₂) and dimethyl carbonate (DMC)) and their effect on the tribological properties of a mineral lubricant. A blend of palm–sesame oil was used to produce biodiesel using ultrasound-assisted transesterification. B30 (30% biodiesel + 70% diesel) fuel was selected as the base fuel. The additives used in the current study to prepare ternary fuel blends were TiO₂ and DMC. B30 + TiO₂ showed a significant reduction of 6.72% in the coefficient of friction (COF) compared to B30. B10 (Malaysian commercial diesel) exhibited very poor lubricity and COF among all tested fuels. Both ternary fuel blends showed a promising reduction in wear rate. All contaminated lubricant samples showed an increment in COF due to the dilution of combustible fuels. Lub + B10 (lubricant + B10) showed the highest increment of 42.29% in COF among all contaminated lubricant samples. B30 + TiO₂ showed the maximum reduction (6.76%) in brake-specific fuel consumption (BSFC). B30 + DMC showed the maximum increment (8.01%) in brake thermal efficiency (BTE). B30 + DMC exhibited a considerable decline of 32.09% and 25.4% in CO and HC emissions, respectively. The B30 + TiO₂ fuel blend showed better lubricity and a significant improvement in engine characteristics.

Keywords: high frequency reciprocating rig; palm-sesame biodiesel; nanoparticle additives; four-ball tribo tester; engine characteristics; tribological characteristics

1. Introduction

Global energy demand is gradually increasing owing to a significant increase in population growth. The transport sector is one of the major consumers of energy, which is the backbone of every country. Around half of the petroleum products are used to fulfil the high energy demand in the transport sector. However, as the fossil fuel reserves deplete gradually, alternative fuels are expected to meet energy demands in future [1]. Among alternative fuels, biodiesel shows a significant reduction in some of the critical exhaust emissions (CO and HC) due to its superior properties such as cetane number, oxygen content, flash point, etc. to those of petroleum-based diesel fuel [2–4]. However, pure biodiesel suffers from poor brake thermal efficiency (BTE) due to lower calorific values which can be alleviated by blending biodiesel with diesel [5,6]. Biodiesel commercialization has some limitations due to poor cold flow properties, higher NO_x emissions, and poor oxidation stability, which can be resolved by mixing different additives such as nanoparticles and oxygenated compounds [7–9]. Malaysia is expected to adopt B30 (30% palm biodiesel in diesel) by 2025 [10]. Indonesia already introduced the B30 biodiesel as of 2020 [11]. At present, Indonesia and Malaysia are exporting palm oil to Asia and Europe for the production of biodiesel to meet energy demands which are expected to increase in future [12]. However, palm oil has very poor cold flow properties because of saturated fatty acids deteriorating its use in cold climate countries [13]. Mujtaba et al. [14] reported that sesame oil (SO) is the best-suited vegetable oil among all other feedstocks for the improvement of cold flow properties, as well as oxidation stability. SO exhibits very good cold flow properties due to high unsaturation. The oxidation stability of SO is higher despite high unsaturation due to antioxidants that occur naturally in SO [15].

The lubricity of fuel is a very important parameter that should be accounted for when selecting fuel for engine applications. Most diesel engine components are self-lubricated with fuel such as the fuel pump, fuel injector, etc. Petroleum diesel has very low lubricity due to the elimination of polar compounds during the desulfurization process [16]. These compounds assist fuel by making a lubricating protective layer between metallic contacts to minimize wear and friction. Lubrication is also very crucial to enhance the overall effectiveness of engine parts [17,18]. The addition of biodiesel in petroleum diesel improves the lubricity of diesel–biodiesel blends which results in lower wear scar diameter (WSD) and coefficient of friction (COF). Few researchers investigated the effect of biodiesel on the lubricity of diesel–biodiesel blends [19–21]. Many researchers used nanoparticles and oxygenated additives with methyl ester and diesel fuel blends to enhance the diesel engine characteristics. Very few studies were carried out on the lubricity of these ternary fuel blends used for improving engine characteristics.

A lubricant film reduces friction and wear; consequently, efficiency increases. According to previous literature, the lubricant is contaminated with fuel up to 5% due to crankcase dilution [20,22]. After dilution, lubricant properties are altered, which directly affects the tribological properties. Few researchers investigated the effect of biodiesel dilution with lubricant on its tribological characteristics [23–25]. Arumugam et al. [26] reported that rapeseed-bio lubricant contaminated with 10% rapeseed biodiesel (B20) fuel showed less wear and friction than commercial synthetic lubricant contaminated with 10% diesel fuel tested using a pin-on-disc apparatus with engine cylinder liner–piston ring combinations. Dhar et al. [19] investigated the tribology of lubricating oil of a diesel engine run on a Karanja biodiesel (B20) blend and mineral-based diesel during an endurance test of 200 h. Their investigation proved that lubricating oil obtained from the biodiesel-fueled engine contained a significantly high amount of wear, trace metals, resinous, ash content, and soot than the lubricating oil from the mineral diesel-fueled engine. Hence, 20% Karanja biodiesel (B20) caused more deterioration of lubricating oil than mineral diesel. Singh et al. [25] also found that more than 5–8% contamination of 100% pure moringa biodiesel fuel in lubricant enhances the lubricity but more than 8% contamination of moringa biodiesel fuel increased the wear rate considerably. Similarly, Maleque et al. [23] and Sulek et al. [24] reported that 5% of biodiesel fuel dilution in commercial lubricant decreased wear rate. A study should be conducted on the contamination of lubricant due to crank dilution with

combustible ternary fuel blends. Many researchers did not pay any attention to lubricant degradation due to dilution with diesel–biodiesel–fuel additives. A tribological study of ternary fuel blends should be conducted before engine application to ensure its effect on degradation of the lubricant.

In this investigation, a 50:50 ratio of palm and SO was used to prepare the biodiesel using ultrasound-assisted transesterification to improve the physicochemical properties (oxidation stability and cold flow properties) of biodiesel. The main objectives of this work were (1) to investigate the lubricity of fuel additives used for enhancement in overall engine characteristics, (2) to investigate the effect of ternary fuel blend contamination with mineral lubricant on its tribological properties, and (3) to investigate the effect of ternary fuel blends on engine performance and emission characteristics.

2. Materials and Methods

Palm oil was procured from Malaysia and SO was obtained from Pakistan. In the current study, a mixture of palm–SO was used to prepare the biodiesel. According to ASTM D6079-11 dimensions, AISI 52100 Chrome hard polished steel balls with a diameter of 6.2 mm, 15-mm SAE-AMS 6440 steel smooth diamond polish discs, and 12.7-mm-diameter AISI 52100 steel balls having hardness 64–66 Rc were procured from the local market.

2.1. Biodiesel Production

A 50:50 ratio of palm–SO was used to prepare the biodiesel using Q500 Sonicator (QSONICA, Newtown, CT, USA) ultrasound equipment as shown in Figure 1. Ultrasound-assisted transesterification was performed under the following operating conditions: time (38.96 min), duty cycle (59.52%), temperature (60 °C), CH₃OH to palm–SO M ratio of 60 vol./vol.%, and potassium hydroxide used as a catalyst with a quantity of 0.70 wt.% [27]. The physicochemical properties of P50S50 biodiesel are presented in Table 1. The physicochemical properties of palm–sesame blend (50:50) methyl esters were estimated in accordance with biodiesel standard methods ASTM D6751 and EN 14214.

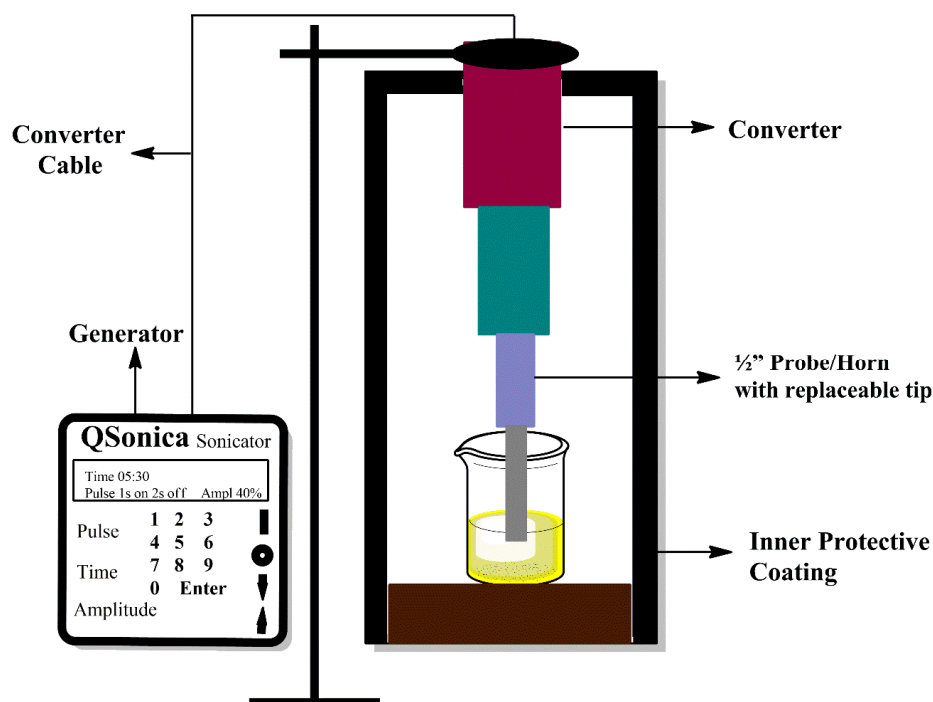


Figure 1. Ultrasound equipment for biodiesel production and sonication of P50S50 blended oil with nanoparticles.

Table 1. Physicochemical properties of P50S50 biodiesel.

Properties of Test Fuel	P50S50	Malaysian Diesel	Equipment	Accuracy
Kinematic viscosity at 40 °C (mm ² /s)	4.43	2.88	SVM 3000, (Anton Paar, Graz, Austria)	±0.35% mm ² /s
Acid Value (mg KOH/g)	0.375	0.152	-	-
Density at 15 °C (kg/m ³)	881	838.96	SVM 3000, (Anton Paar, Graz, Austria)	±0.1 kg/m ³
High heating value (MJ/kg)	41.24	45.67	C2000 basic calorimeter, IKA, Staufen, Germany	±0.1% MJ/kg
Cetane number	53.37	48.50	-	-
Cold filter plugging point (°C)	-1.714	0	CFFP NTL 450, Compass Instruments, IL, USA	-
Flash point (°C)	>151	77.90	Pensky-Martens closed cup tester NPM 440, Normalab, Valliquerville, France	±0.1 °C
Cloud point (°C)	7.82	2.05	Cloud and pour point tester NTE 450, Normalab, Valliquerville, France	±0.1 °C
Pour point (°C)	3.821	2.1	Cloud and pour point tester NTE 450, Normalab, Valliquerville, France	-
Oxidation stability (h)	6.89	13.20	873 Biodiesel Rancimat, Metrohm, Herisau, Switzerland	±0.01 h

2.2. Fuel Samples Preparation

2.2.1. Fuel Sample Preparation for HFRR and Engine Test Rig

Various fuel samples were prepared to study the lubricity of fuel and the effect of ternary fuel blends on diesel engine characteristics. The prepared fuel samples were compared with commercially available Malaysian diesel (B10). Pure B100 biodiesel was produced using the ultrasound technique. Then, 20% P50S50 biodiesel was mixed with Malaysian commercial diesel to prepare the B30 fuel blend. Additionally, two ternary fuel additive blends were prepared to study the tribological behavior. B30 fuel was mixed with 20% dimethyl carbonate (DMC) (by volume) and stirred at a standard speed 2000 rpm for half an hour to achieve a homogeneous blend. Ultrasound Sonicator Q500 Sonicator (QSONICA, Newtown, USA) as shown in Figure 1 was used to prepare the nanoparticle (TiO₂) and B30 ternary fuel blend. The B30 with 100 ppm TiO₂ nanoparticle fuel sample was prepared at a stirring speed of 900 rpm for 30 min on a magnetic stirrer and sonicated to disperse the nanoparticles at a frequency of 20 Hz for 20 min at an amplitude of 30%. The physicochemical properties were measured and are shown in Table 2.

Table 2. Properties of tested fuel samples. DMC—dimethyl carbonate.

Test Fuel Blends	Density at 15 °C	Kinematic Viscosity at 40 °C	Calorific Value	Viscosity Index
	kg/m ³	mm ² /s	MJ/kg	
B10	855.9	3.153	43.92	81.2
B100 (P50S50 biodiesel)	880	4.420	41.25	186.2
B30	852.6	3.348	43.14	164.2
B30 + DMC	878	2.457	39.78	-
B30 + TiO ₂	853	3.364	42.93	208.3

2.2.2. Lubricant Sample Preparation

Firstly, 5% of each of the above-mentioned fuels in Table 2 was mixed with commercial lubricant SAE-40 using a magnetic stirrer at 900 rpm speed for 30 min, as 5% lubricant mixing with fuel happened due to dilution of the crankcase. The physicochemical properties of reference lubricant SAE-40 and all other lubricant samples with different fuels were measured using the viscometer (SVM 3000) as shown in Table 3.

Table 3. Physicochemical properties of tested lubricant fuel samples.

Lubricant Samples	Physicochemical Properties of Lubricant Samples		
	Density at 15 °C (kg/m ³)	Viscosity at 40 °C (mm ² /s)	Viscosity Index
100% Lubricant (SAE 40)	873.7	87,022	201.3
Lubricant + 5% B10	872.0	71,072	205.3
Lubricant + 5% B30	873.3	76,652	221.6
Lubricant + 5% B30 + DMC	872.0	64,509	-
Lubricant + 5% B30 + TiO ₂	872.1	69,311	205.4

2.3. Experimental Set-Up

2.3.1. Diesel Engine Set-Up

The Yanmar (TF 120M) single-cylinder and radiator cooled diesel engine as shown in Figure 2 was used to study the effect of ternary fuel blends on diesel engine performance and emission characteristics. The diesel engine parameters were as follows: maximum power (7.7 kW), compression ratio (17.7), maximum rpm (2400 rpm), injection timing (17° before top dead center (BTDC)), and injection pressure (200 kg/cm²). The emissions of the engine exhaust gases such as CO, HC, and NO_x were measured utilizing the BOSCH BEA 350 gas analyzer. All experiments were done in triplicate. Error bars are presented along with the data points in the figures. The accuracies of the measurements for diesel engine characteristics are mentioned in Table 4. The overall uncertainty of diesel engine experiments was calculated using Equation (1).

$$\begin{aligned}
 \text{Overall uncertainty} &= \sqrt{\text{Uncertainty \% of } (\text{BSFC}^2 + \text{BTE}^2 + \text{BP}^2 + \text{CO}^2 + \text{NO}_x^2 + \text{HC}^2)} \\
 &= \sqrt{((1.31)^2 + (0.324)^2 + (0.667)^2 + (1)^2 + (1.3)^2 + (1)^2)} \\
 &= \pm 2.44\%.
 \end{aligned}
 \tag{1}$$

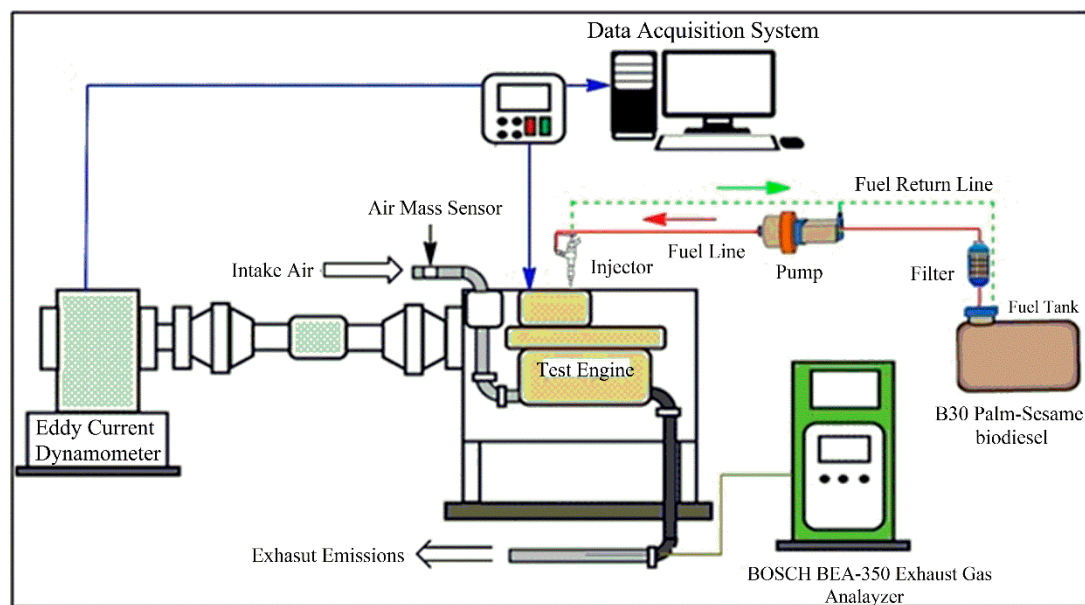
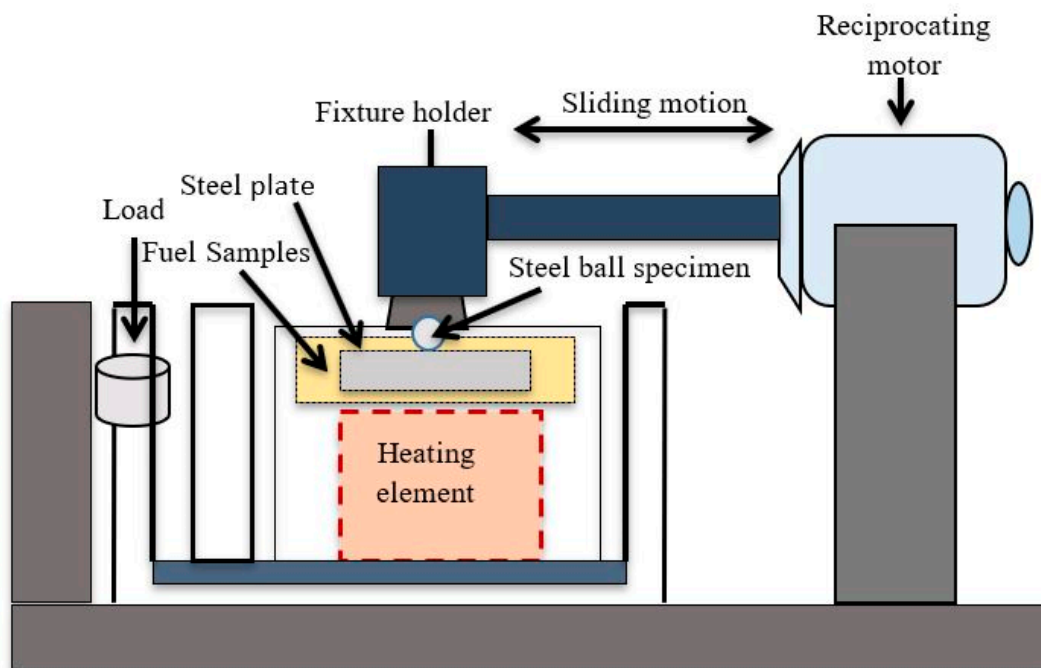
**Figure 2.** Schematic view of diesel engine set-up.

Table 4. Accuracies of measurements used for experiments.

Measurement	Measurement Range	Accuracy (\pm)
Speed	60–10,000 rpm	± 10 rpm
Load	± 120 Nm	± 0.1 Nm
Flow Measurement	0.5–36 L/h	± 0.01 L/h
CO	0–10 vol.%	± 0.001 vol.%
HC	0–9999 ppm	± 1 ppm
NOx	0–5000 ppm	± 1 ppm

2.3.2. HFRR Test Rig

HFRR equipment from DUCOM (Model: TR-281-M8) as shown in Figure 3 was used to study the lubricity of tested fuel samples. The testing specimen plates were prepared by cutting 15 mm \times 15 mm pieces. The specimens were polished with silicon carbide papers using the polishing machine. A ball on a test specimen plate was used to analyze the tribological behavior of fuel samples. Steel ball slides on the steel specimen plate were submerged in 5.0 \pm 0.2 mL of fuel sample in a reciprocating motion with 2.0 \pm 0.02 mm stroke length at a frequency 10.0 \pm 1 Hz for 70 min with an applied load of 5 \pm 0.01 N. Fuel temperature was constant at 60 \pm 2 $^{\circ}$ C during the tribology test. All operating conditions followed the standard test method ASTM D6079-11.

**Figure 3.** Schematic view of HFRR test rig.

2.3.3. Four-Ball Tribo Tester Rig

An automatic four-ball tribo tester (FBT-3, Ducom Instruments, Bengaluru, India) as shown in Figure 4 was used to study the effect of different fuels on lubricant tribological characteristics. Then, 10 mL of lubricant sample was poured into the cup holder containing three stationary steel balls attached to the temperature sensor. For each experiment, four new separate steel balls were used. Commercial lubricant SAE-40 was also tested as a reference lubricant for comparing the results. All experiments were performed according to the ASTM D4172 standard; the working conditions were as follows: test duration (60 min), applied load (40 kg), oil temperature (60 $^{\circ}$ C), and rotational speed of spindle (1200 rpm).

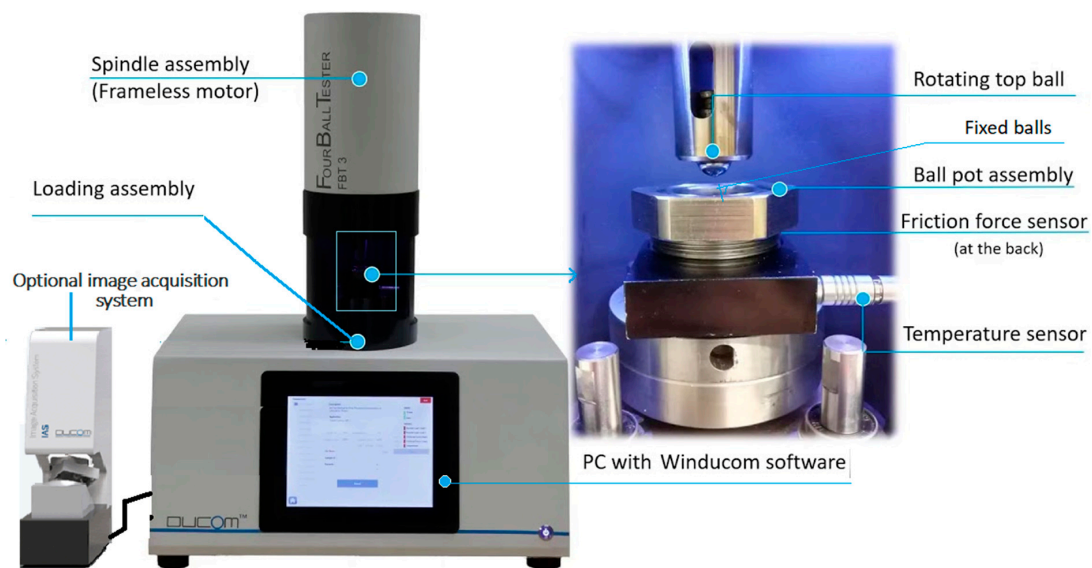


Figure 4. Schematic view of four-ball tribo tester rig.

3. Results and Discussion

3.1. Engine Performance

Brake-specific fuel consumption (BSFC) and BTE results for fuel samples at full load condition with variable engine speed are presented in Figure 5a,b. The BSFC values of various tested fuel samples, i.e., B10, B30, B30 + TiO₂, and B30 + DMC, were 0.373 kg/kWh, 0.384 kg/kWh, 0.403 kg/kWh, and 0.407 kg/kWh, respectively, at 2050 rpm are shown in Figure 5a. On average, the B30 + TiO₂ ternary blend exhibited the lowest BSFC among all the tested fuels. The average BSFC value of B30 + DMC decreased compared to B30 but increased in comparison to B10 due to a lower heating value [28]. Ternary fuel blends showed improvements in BSFC reduction of 6.76% and 1.45% for B30 + TiO₂ and B30 + DMC in comparison with B30. The lower BSFC in the case of an alcoholic ternary blend was due to lower viscosity and density which improved the fuel spray characteristics and led to a better A:F mixture due to enhanced atomization [29,30]. The higher evaporation rate of alcoholic ternary blends resulted in enhanced combustion properties and better fuel spray characteristics. The nanoparticle ternary fuel blend showed a significant reduction in BSFC due to a lower ignition delay that led to less premixed combustion of air and fuel mixture [31]. The nanoparticles as fuel improvers avoided the deposition of carbon and iron particles, resulting in decreased friction among diesel engine components, thus leading to an increase in BP and torque along with a reduction in BSFC.

Figure 5b exhibits the effect of speed on BTE. On average, 8.01% and 5.49% increments in BTE values were noted for the B30 blend with additives DMC and TiO₂, respectively, in comparison with neat B30 fuel. There was an enhancement in the BTE value when the alcohol fuel additive was added, which acted as an oxygen donor due to a reduction in combustion time and enhanced combustion process [32]. The thermal efficiency of diesel–biodiesel–fuel additive blends improved due to improved combustion with a supply of excess oxygen in the fuel-rich zone in the compression ignition engine combustion chamber [30,33]. TiO₂ nanoparticles enhanced the density of fuel–air charge due to the high evaporation rate of fuel which resulted in higher power and BTE [34]. A higher BTE value was observed because of the addition of titanium oxide nanoparticles as a nano fuel additive, which have a high chemical reactive surface and surface volume ratio, thereby boosting the combustion by proving better oxidation. Similar results reported by various researchers. Örs et al. [35] reported a 24.52% improvement in the BSFC of B20 blend with the addition of TiO₂ compared to B20 and the average reduction in the BSFC for B20 with TiO₂ was 27.73%. Silva et al. [36] also found a 21.28% reduction in BSFC due to the addition of TiO₂ nanoparticles compared to petroleum diesel. Yuvarajan Devarajan [37]

showed a 4.1% reduction in BSFC and a 1.6% increment in BTE with the addition of 20% DMC to biodiesel blends.

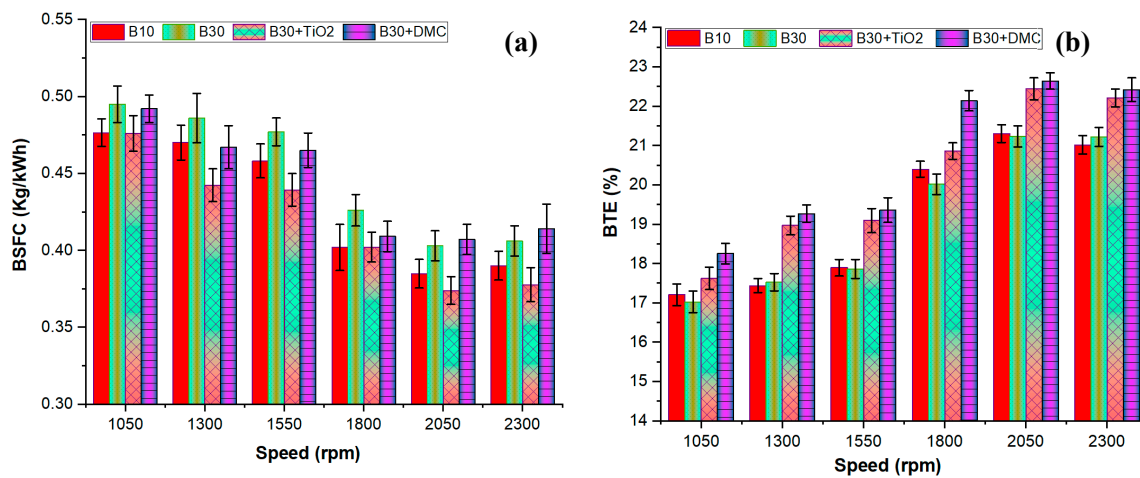


Figure 5. Variation of engine performance parameters: (a) brake-specific fuel consumption (BSFC) and (b) brake thermal efficiency (BTE) with respect to speed at 100% engine load.

3.2. Engine Emissions

Exhaust emission (HC, NO_x, and CO) results for tested fuel samples are exhibited in Figure 6a–c. The formation of CO emissions is mainly dependent on the combustion process. Incomplete combustion leads to CO formation. The presence of oxygen molecules in fuel assists in the completion of the combustion process and conversion of CO to CO₂. From Figure 6a, it is evident that CO emissions reduced significantly in the case of biodiesel–diesel and for the alcohol and nano fuel blends in comparison to the standard commercially used Malaysian (B10) diesel. All ternary blends showed an average significant reduction in CO emissions with the addition of fuel additives, with 32.09% and 12.46% for B30 with the fuel additives DMC and TiO₂, respectively, in comparison with the B30 blend. In another study conducted by Örs et al. [35], it was observed that the addition of TiO₂ reduced the CO emissions by 10.83% and 25.56% for B20 with TiO₂ compared to B20 and petroleum diesel, respectively. The same observation was found by Saxena et al. [38]. A 7.4% reduction in CO emissions was reported by Yuvarajan Devarajan [37] with the addition of 20% DMC to the fuel blend. The oxygenated alcohol ternary blend showed a remarkable reduction in CO emissions due to the presence of a high amount of oxygen content compared to other fuel samples. Nanoparticle ternary fuel blends also reduced CO emissions due to the potential redox active property that assisted in the complete conversion of CO to CO₂ [39]. The chemical reactive surface of nanoparticles due to a higher surface volume reduces the ignition delay, resulting in a better combustion process and consequently reducing CO emissions [40].

Figure 6b exhibits the trend of HC emissions with respect to engine speed. Similarly, incomplete combustion is the source of HC emissions. The reduction in HC emissions was due to high oxygen content and a higher cetane number of ternary fuel blends, which resulted in lower ignition delay [41]. All ternary blends and the B30 fuel sample showed a substantial decline in hydrocarbon emissions in comparison to B10. B30 fuel blended with DMC and titanium dioxide fuel additives showed reductions in HC emissions by 25.4% and 8.63%, respectively, in comparison with the neat B30 fuel, due to higher oxygen content. An average reduction in HC emissions of 34.12% for B20 with TiO₂ was reported by Örs et al. [35]. In another study [37], the addition of DMC (20%) as a fuel additive minimized the HC emissions by up to 5.2%. The larger surface area of nanoparticles and higher oxygen amount in ternary fuel blends improved the fuel combustion process, which led to lower HC emissions. Oxygenated ternary fuel blends increased the in-cylinder pressure and temperature and heat release rate, which resulted in the improved combustion process and lower HC emissions [42]. Nanoparticles

accelerated the oxidation process of hydrocarbons into CO_2 and water, consequently reducing HC emissions [43].

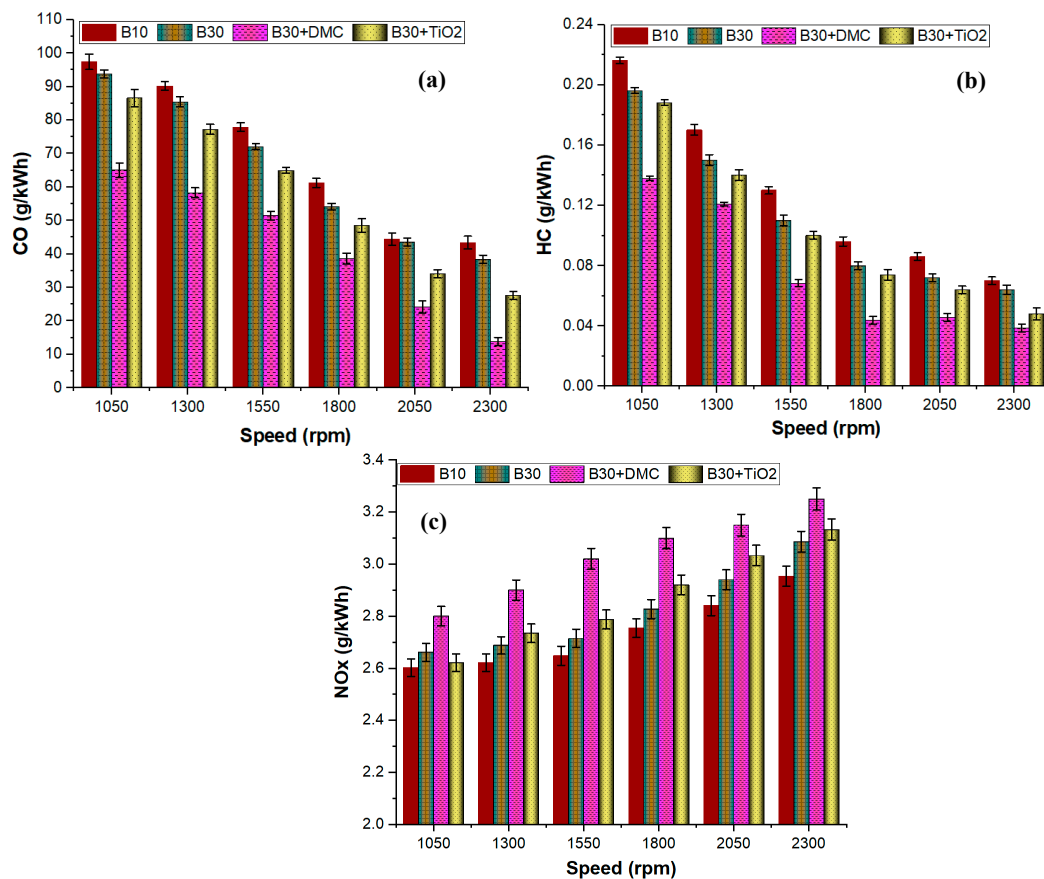


Figure 6. Variation of engine exhaust emissions: (a) CO, (b) HC, and (c) NOx with respect to speed at 100% engine load.

Figure 6c represents the NOx emissions for all tested fuel samples. Ternary fuel samples showed an increment in NOx emissions compared to B10 and B30. The test fuel blends demonstrated an increase in NOx emissions by 9.72% and 1.84% for B30 fuel blended with DMC and titanium dioxide fuel additives in comparison with the neat B30 fuel. The higher oxygen content and cetane number of ternary fuel blends increased the in-cylinder temperature and pressure, which led to higher NOx emissions. A similar increment in NOx emissions was reported in B20 with TiO_2 up to 6.95% compared to B20 [35]. Significant increments in NOx emissions were observed with the addition of DMC (10% and 20%) to fuel blends compared to petroleum diesel [42]. The oxygenated ternary fuel blend contained a higher amount of oxygen content among all tested fuels, which resulted in high in-cylinder combustion temperature and pressure, consequently increasing NOx emissions [44]. Nanoparticle ternary fuel blends improved the combustion process by providing excess oxygen, which resulted in a high combustion temperature and higher NOx. The higher thermal conductivity and large surface area of nanoparticles increased the in-cylinder pressure and enhanced the combustion process, resulting in higher NOx emissions [40].

3.3. HFRR Tribological Study

The COF and WSD results of all five tested fuel samples are exhibited in Figure 7a,b. The lubricity of fuel is a very important factor that should be considered before the application of fuel in the automotive industry. Engine life is mainly dependent on the lubricity of the fuel. Diesel engine components (fuel pump, fuel injector, etc.) are self-lubricated with the fuel itself. The COF trend with

respect to time is presented in Figure 7a. During the early stage of the experiment, all tested fuels showed a sharp rise in COF for a few minutes, named the run-in period. During this period, there is no lubricating film between mating surfaces, leading to very high COF. After this run-in period, steady-state conditions are achieved due to the formation of a thin lubricating protective layer between metallic surfaces. B10 (Malaysian commercial diesel) showed a higher COF value than all fuel samples due to a lower percentage of ester molecules compared to other fuel samples. The unsteady state for B10 (Malaysian commercial diesel) increased with time compared to other samples because B30 with fuel additives had a shorter run-in period due to the presence of ester molecules and nanoparticles that created a protective layer quickly compared to B10. The ester molecules in fuel samples assisted in the formation of the protective lubricating film between mating surfaces [45]. The pure biodiesel fuel sample showed a minimum run-in period due to the adsorption of ester molecules on the metallic surface, which acted as a protective layer during the rubbing process. B30 and B30 with fuel additives showed a significant reduction in COF values compared to B10 because of ester molecules and nanoparticles which acted as a protective layer between mating surfaces. From Figure 7b, it is evident that pure biodiesel showed the lowest average COF value among all tested fuel samples. The higher percentage of unsaturated fatty acids in the biodiesel sample improved the lubricity of fuel and resulted in lower COF and WSD. Among all tested fuel blends, B30 + TiO₂ showed a significant reduction in COF due to the presence of spherical-shape nanoparticles that acted as a surfactant between metallic surfaces. Nanoparticles also acted as a ball bearing between rubbing surfaces, consequently reducing COF and WSD. The alcoholic ternary blend exhibited the highest COF value amongst all the fuel blends except for B10. B30 blended with DMC fuel contained a higher amount of oxygen content, which led to the lowest WSD among all tested fuels due to the formation of an anti-adhesive oxide layer between metallic surfaces at the initial stage of the experiment. On average, B30 + TiO₂ showed a reduction of 6.72% and B30 + DMC exhibited an increment of 7.15% in COF in comparison to B30 fuel. Both ternary blends showed a significant reduction in WSD by 38.4% and 23.5% for B30 fuel blended with DMC and TiO₂ fuel additives in comparison with the neat B30 fuel blend.

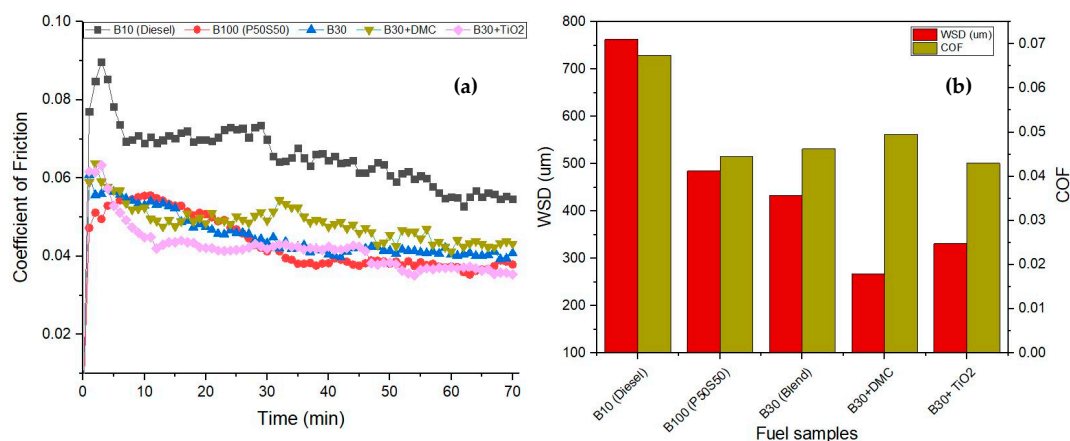


Figure 7. Coefficient of friction (a)(COF) and (b)wear scar diameter (WSD) trend for all tested fuel samples.

3.4. Four-Ball Tribological Study

The effect of different fuel samples on the lubricity of mineral lubricant is presented in Figure 8a,b. According to previous literature, the lubricant is contaminated with fuel up to 5% due to crankcase dilution [20]. The lubricant was contaminated with combustible fuel which altered the tribological properties of lubricant and resulted in poor lubricating characteristics due to lubricant degradation. Figure 8a exhibits the friction coefficient trend for all tested samples. The run-in period of pure mineral lubricant was much lower due to better lubricating characteristics. Steady-state conditions were achieved quickly due to the formation of the lubricating film between metallic contacts in the initial

phase of the experimental run [46]. The mineral lubricant showed a much lower COF compared to other contaminated samples of lubricant with different fuels. The addition of combustible fuel to the lubricant altered its lubricating properties and resulted in poor tribological behavior. It is also evident from Figure 8a that mineral lubricant contaminated with a higher percentage of biodiesel fuel sample (B30) and B30 with fuel additives showed less lubricant degradation compared to B10. The lubricant + B10 sample showed the highest COF value among all tested samples because of a higher percentage of diesel in the sample compared to other tested samples. All contaminated lubricant samples showed high COF due to a decrease in viscosity, which had a high influence on the lubricity of fuel compared to mineral lubricant. Among ternary contaminated samples, Lub + B30 + TiO₂ showed the best friction coefficient due to the presence of nanoparticles which acted as a surface between metallic contacts and resulted in lower COF compared to other contaminated lubricant samples. Figure 8b presents the average results of COF and WSD for all tested samples. Lub + B10 showed the highest COF value among all tested samples due to the presence of high sulfur content and a low percentage of ester molecules, which resulted in a poor lubricating film between metallic contacts, consequently increasing COF and WSD. On average, Lub + B30 + TiO₂ exhibited the lowest COF value among all contaminated lubricant samples due to the presence of spherical-shape nanoparticles which acted as a friction-reducing agent between rubbing surfaces. Lub + B30 also showed a lower COF compared to Lub + B10 due to the presence of a high amount of ester molecules. Yashvir Singh et al. [25] also found that more than 5–8% contamination of 100% pure moringa biodiesel fuel in lubricant enhanced the lubricity, but more than 8% contamination of moringa biodiesel fuel increased the wear rate considerably. Similarly, Maleque et al. [23] and Sulek et al. [24] reported that 5% biodiesel fuel dilution in commercial lubricant decreased the wear rate. All contaminated samples showed increments in COF of 13.72%, 27%, 31.35%, and 42.29% for Lub + B30 + TiO₂, Lub + B30 + DMC, and Lub + B10, respectively, compared to mineral lubricant. All contaminated lubricant samples showed lower WSD values compared to mineral lubricant due to the presence of ester molecules, long-chain carbon atoms, and fuel additives (oxygenated alcohols and nanoparticles), which acted as a surfactant between metallic contacts. On average, WSD values decreased by 28.9%, 25.24%, 24.25%, and 17% for Lub + B30, Lub + B30 + DMC, Lub + B30 + TiO₂, and Lub + B10, respectively, compared to mineral lubricant.

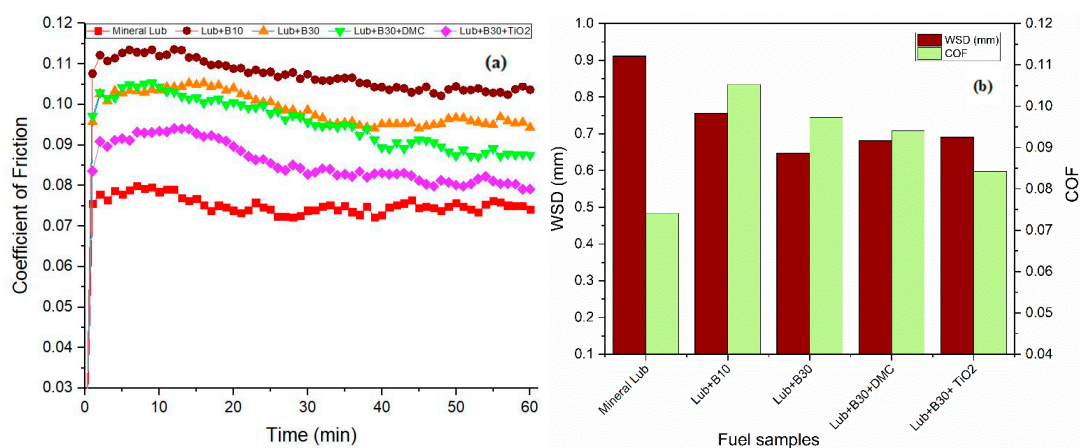


Figure 8. Tribological behavior: (a) COF and (b) WSD of mineral lubricant and lubricant contaminated samples.

4. Conclusions

In this current study, palm–sesame biodiesel was produced, and various biodiesel–diesel–fuel additive blends were prepared to examine their lubricity, as well as the effect of these blends on the contamination of lubricant and the effect of ternary fuel blends on diesel engine characteristics. Based on the results obtained, the conclusions below were made.

1. B10 (Malaysian commercial diesel) presented very poor lubricity. The B10 fuel blend showed very high COF and WSD values compared to other tested fuels.
2. On average, B30 + TiO₂ showed a reduction of 6.72% and B30 + DMC exhibited an increment of 7.15% in COF in comparison to B30 fuel. Both fuel additive blends showed a significant reduction in WSD by 38.4% and 23.5% for B30 fuel blended with DMC and TiO₂ fuel additives in comparison with the neat B30 fuel blend.
3. All contaminated samples showed increments in COF of 13.72%, 27%, 31.35%, and 42.29% for Lub + B30 + TiO₂, Lub + B30 + DMC, and Lub + B10, respectively, compared to mineral lubricant.
4. Ternary test fuels demonstrated an improvement in BSFC reduction of 6.76% and 1.45% for B30 fuel blended with DMC and TiO₂ fuel additives in comparison with the neat B30 fuel blend.
5. All ternary test fuels demonstrated a significant reduction in emissions of carbon monoxide upon adding fuel additives by 32.09% and 12.46% for B30 fuel blended with DMC and TiO₂, respectively, in comparison with the B30 fuel blend.
6. The B30 fuel blended with DMC and TiO₂ nanoparticles showed a reduction in HC emissions of 25.4% and 8.63%, respectively, compared to B30 due to the presence of higher oxygen content.
7. On average, the blends with fuel additives resulted in an increase in NO_x emissions by 9.72% and 1.84% for B30 fuel blended with DMC and TiO₂ in comparison with the B30 fuel blend.

The main findings of this current research work are that Malaysian commercial diesel showed poor tribological characteristics, while the nanoparticle (TiO₂) blended fuel showed the best lubricity among all tested fuel samples. The oxygenated alcohol (DMC) blended fuel showed better engine performance and emission (HC and CO) characteristics among all tested fuel samples.

5. Future Recommendations

Finally, we suggest that nanoparticles as fuel additives are more feasible due to their promising results. TiO₂ nanoparticles showed a significant reduction in COF compared to oxygenated alcoholic fuel additives. TiO₂ nanoparticles acted as a friction-reducing agent due to their spherical shape, which established a thin lubricating film between metallic contacts, consequently reducing COF. In the future, a long endurance test should be conducted to investigate the effect of fuel additives and lubricant contamination on the diesel engine components.

Author Contributions: Conceptualization, M.A.M and M.A.K.; methodology, M.A.M.; validation, L.R., F.N., and M.F.; formal analysis, M.G.; investigation, M.A.M., S.B., and M.E.M.S.; writing—original draft preparation, M.A.M.; writing—review and editing, I.M.R.F. and H.C.O.; supervision, H.H.M. All authors read and agreed to the published version of the manuscript.

Funding: The authors take the opportunity to thank the UNIVERSITY OF MALAYA for the financial support under research grant FP142-2019A under the FRGS from the University of Malaya, Kuala Lumpur, Malaysia, and HEC ISLAMABAD, PAKISTAN for supporting the research under Grant No. 5-1/HRD/UESTPI (Batch-VI)/4954/2018/HEC.

Acknowledgments: The authors also acknowledge the contribution of the research development fund of the School of Information, Systems, and Modeling, University of Technology Sydney, Australia.

Conflicts of Interest: The authors declare no conflict of interest.

Nomenclature

ASTM	American Standard for Testing Materials
B100	100% biodiesel
EN	Europe Union
CI	Compression ignition
B30	70% diesel + 30% biodiesel

KOH	Potassium hydroxide
B10	10% biodiesel + 90% diesel
BTE	Brake thermal efficiency
HFRR	High-frequency reciprocating rig
BSFC	Brake-specific fuel consumption
TiO ₂	Titanium oxide
BTDC	Before top dead center
P50S50	50% palm and 50% sesame
SO	Sesame oil
B30 + TiO ₂	70% diesel + 30% biodiesel + 100 ppm TiO ₂ by mass
COF	Coefficient of friction
ppm	Parts per million
HC	Hydrocarbon
DMC	Dimethyl carbonate
CO	Carbon monoxide
WSD	Wear scar diameter
NO _x	Nitrogen oxides

References

- Fattah, I.M.R.; Ong, H.C.; Mahlia, T.M.I.; Mofijur, M.; Silitonga, A.S.; Rahman, S.M.A.; Ahmad, A. State of the Art of Catalysts for Biodiesel Production. *Front. Energy Res.* **2020**, *8*. [[CrossRef](#)]
- Ong, H.C.; Milano, J.; Silitonga, A.S.; Hassan, M.H.; Shamsuddin, A.H.; Wang, C.-T.; Indra Mahlia, T.M.; Siswanto, J.; Kusumo, F.; Sutrisno, J. Biodiesel production from Calophyllum inophyllum-Ceiba pentandra oil mixture: Optimization and characterization. *J. Clean. Prod.* **2019**, *219*, 183–198. [[CrossRef](#)]
- Silitonga, A.; Shamsuddin, A.; Mahlia, T.; Milano, J.; Kusumo, F.; Siswanto, J.; Dharma, S.; Sebayang, A.; Masjuki, H.; Ong, H.C. Biodiesel synthesis from Ceiba pentandra oil by microwave irradiation-assisted transesterification: ELM modeling and optimization. *Renew. Energy* **2020**, *146*, 1278–1291. [[CrossRef](#)]
- Ong, H.C.; Masjuki, H.H.; Mahlia, T.M.I.; Silitonga, A.S.; Chong, W.T.; Yusaf, T. Engine performance and emissions using Jatropha curcas, Ceiba pentandra and Calophyllum inophyllum biodiesel in a CI diesel engine. *Energy* **2014**, *69*, 427–445. [[CrossRef](#)]
- Gad, M.S.; Jayaraj, S. A comparative study on the effect of nano-additives on the performance and emissions of a diesel engine run on Jatropha biodiesel. *Fuel* **2020**, *267*, 117168. [[CrossRef](#)]
- Mahlia, T.M.I.; Syazmi, Z.A.H.S.; Mofijur, M.; Abas, A.E.P.; Bilad, M.R.; Ong, H.C.; Silitonga, A.S. Patent landscape review on biodiesel production: Technology updates. *Renew. Sustain. Energy Rev.* **2020**, *118*, 109526. [[CrossRef](#)]
- Silitonga, A.S.; Masjuki, H.H.; Mahlia, T.M.I.; Ong, H.C.; Chong, W.T.; Boosroh, M.H. Overview properties of biodiesel diesel blends from edible and non-edible feedstock. *Renew. Sustain. Energy Rev.* **2013**, *22*, 346–360. [[CrossRef](#)]
- Imtenan, S.; Masjuki, H.H.; Varman, M.; Rizwanul Fattah, I.M.; Sajjad, H.; Arbab, M.I. Effect of n-butanol and diethyl ether as oxygenated additives on combustion–emission–performance characteristics of a multiple cylinder diesel engine fuelled with diesel–jatropha biodiesel blend. *Energy Convers. Manag.* **2015**, *94*, 84–94. [[CrossRef](#)]
- Fattah, I.M.R.; Masjuki, H.H.; Kalam, M.A.; Wakil, M.A.; Ashraful, A.M.; Shahir, S.A. Experimental investigation of performance and regulated emissions of a diesel engine with Calophyllum inophyllum biodiesel blends accompanied by oxidation inhibitors. *Energy Convers. Manag.* **2014**, *83*, 232–240. [[CrossRef](#)]
- Latiff, R. *Malaysia to Implement B30 Biodiesel Mandate in Transport Sector before 2025*; Sarkar, H., Ed.; REUTERS: Putrajaya, Malaysia, 2020.
- Elisha, O.; Fauzi, A.; Anggraini, E. Analysis of Production and Consumption of Palm-Oil Based Biofuel using System Dynamics Model: Case of Indonesia. *Int. J. Sci. Eng. Technol.* **2019**, *6*. [[CrossRef](#)]
- Coca, N. *As Palm Oil for Biofuel Rises in Southeast Asia, Tropical Ecosystems Shrink*; Chinadialogue China: Beijing, China, 2020.

13. Fattah, I.M.R.; Masjuki, H.H.; Kalam, M.A.; Mofijur, M.; Abedin, M.J. Effect of antioxidant on the performance and emission characteristics of a diesel engine fueled with palm biodiesel blends. *Energy Convers. Manag.* **2014**, *79*, 265–272. [[CrossRef](#)]
14. Mujtaba, M.A.; Muk Cho, H.; Masjuki, H.H.; Kalam, M.A.; Ong, H.C.; Gul, M.; Harith, M.H.; Yusoff, M.N.A.M. Critical review on sesame seed oil and its methyl ester on cold flow and oxidation stability. *Energy Rep.* **2020**, *6*, 40–54. [[CrossRef](#)]
15. Mujtaba, M.A.; Masjuki, H.H.; Kalam, M.A.; Ong, H.C.; Gul, M.; Farooq, M.; Soudagar, M.E.M.; Ahmed, W.; Harith, M.H.; Yusoff, M.N.A.M. Ultrasound-assisted process optimization and tribological characteristics of biodiesel from palm-sesame oil via response surface methodology and extreme learning machine-Cuckoo search. *Renew. Energy* **2020**. [[CrossRef](#)]
16. Gul, M.; Masjuki, H.H.; Kalam, M.A.; Zulkifli, N.W.M.; Mujtaba, M.A. A Review: Role of Fatty Acids Composition in Characterizing Potential Feedstock for Sustainable Green Lubricants by Advance Transesterification Process and its Global as Well as Pakistani Prospective. *BioEnergy Res.* **2020**, *13*, 1–22. [[CrossRef](#)]
17. Lapuerta, M.; García-Contreras, R.; Agudelo, J.R. Lubricity of Ethanol-Biodiesel-Diesel Fuel Blends. *Energy Fuels* **2010**, *24*, 1374–1379. [[CrossRef](#)]
18. Liaquat, A.M.; Masjuki, H.H.; Kalam, M.A.; Rizwanul Fattah, I.M. Impact of biodiesel blend on injector deposit formation. *Energy* **2014**, *72*, 813–823. [[CrossRef](#)]
19. Dhar, A.; Agarwal, A.K. Experimental investigations of effect of Karanja biodiesel on tribological properties of lubricating oil in a compression ignition engine. *Fuel* **2014**, *130*, 112–119. [[CrossRef](#)]
20. Arumugam, S.; Sriram, G. Preliminary study of nano-and microscale TiO₂ additives on tribological behavior of chemically modified rapeseed oil. *Tribol. Trans.* **2013**, *56*, 797–805. [[CrossRef](#)]
21. Agarwal, A.K. Lubricating Oil Tribology of a Biodiesel-Fuelled Compression Ignition Engine. Proceedings of ASME 2003 Internal Combustion Engine Division Spring Technical Conference, Erie, PA, USA, 7–10 September 2003.
22. Gul, M.; Zulkifli, N.W.M.; Masjuki, H.H.; Kalam, M.A.; Mujtaba, M.A.; Harith, M.H.; Syahir, A.Z.; Ahmed, W.; Bari Farooq, A. Effect of TMP-based-cottonseed oil-biolubricant blends on tribological behavior of cylinder liner-piston ring combinations. *Fuel* **2020**, *278*, 118242. [[CrossRef](#)]
23. Maleque, M.A.; Masjuki, H.H.; Haseeb, A.S.M.A. Effect of mechanical factors on tribological properties of palm oil methyl ester blended lubricant. *Wear* **2000**, *239*, 117–125. [[CrossRef](#)]
24. Sulek, M.; Kulczycki, A.; Malysa, A. Assessment of lubricity of compositions of fuel oil with biocomponents derived from rape-seed. *Wear* **2010**, *268*, 104–108. [[CrossRef](#)]
25. Singh, Y.; Singla, A.; Upadhyay, A.; Singh, A.K. Sustainability of Moringa-oil-based biodiesel blended lubricant. *Energy Sources Part A: Recovery Util. Environ. Eff.* **2017**, *39*, 313–319. [[CrossRef](#)]
26. Arumugam, S.; Sriram, G. Effect of Bio-Lubricant and Biodiesel-Contaminated Lubricant on Tribological Behavior of Cylinder Liner–Piston Ring Combination. *Tribol. Trans.* **2012**, *55*, 438–445. [[CrossRef](#)]
27. Mofijur, M.; Kusumo, F.; Fattah, I.; Mahmudul, H.; Rasul, M.; Shamsuddin, A.; Mahlia, T. Resource Recovery from Waste Coffee Grounds Using Ultrasonic-Assisted Technology for Bioenergy Production. *Energies* **2020**, *13*, 1770. [[CrossRef](#)]
28. Mofijur, M.; Masjuki, H.H.; Kalam, M.A.; Atabani, A.E.; Fattah, I.M.R.; Mobarak, H.M. Comparative evaluation of performance and emission characteristics of Moringa oleifera and Palm oil based biodiesel in a diesel engine. *Ind. Crop. Prod.* **2014**, *53*, 78–84. [[CrossRef](#)]
29. Murcak, A.; Haşimoğlu, C.; Çevik, İ.; Karabektaş, M.; Ergen, G. Effects of ethanol–diesel blends to performance of a DI diesel engine for different injection timings. *Fuel* **2013**, *109*, 582–587. [[CrossRef](#)]
30. Imtenan, S.; Masjuki, H.H.; Varman, M.; Rizwanul Fattah, I.M. Evaluation of n-butanol as an oxygenated additive to improve combustion-emission-performance characteristics of a diesel engine fuelled with a diesel-calophyllum inophyllum biodiesel blend. *RSC Adv.* **2015**, *5*, 17160–17170. [[CrossRef](#)]
31. Nadeem, M.; Rangkuti, C.; Anuar, K.; Haq, M.; Tan, I.; Shah, S. Diesel engine performance and emission evaluation using emulsified fuels stabilized by conventional and gemini surfactants. *Fuel* **2006**, *85*, 2111–2119. [[CrossRef](#)]
32. Khalife, E.; Tabatabaei, M.; Demirbas, A.; Aghbashlo, M. Impacts of additives on performance and emission characteristics of diesel engines during steady state operation. *Prog. Energy Combust. Sci.* **2017**, *59*, 32–78. [[CrossRef](#)]

33. Imtenan, S.; Varman, M.; Masjuki, H.H.; Kalam, M.A.; Sajjad, H.; Arbab, M.I.; Fattah, I.M.R. Impact of low temperature combustion attaining strategies on diesel engine emissions for diesel and biodiesels: A review. *Energy Convers. Manag.* **2014**, *80*, 329–356. [[CrossRef](#)]
34. Anbarasu, A.; Karthikeyan, A. Performance and emission characteristics of a diesel engine using cerium oxide nanoparticle blended biodiesel emulsion fuel. *J. Energy Eng* **2016**, *142*, 04015009. [[CrossRef](#)]
35. Örs, I.; Sarıkoç, S.; Atabani, A.E.; Ünalın, S.; Akansu, S.O. The effects on performance, combustion and emission characteristics of DICl engine fuelled with TiO₂ nanoparticles addition in diesel/biodiesel/n-butanol blends. *Fuel* **2018**, *234*, 177–188. [[CrossRef](#)]
36. D’Silva, R.; Binu, K.; Bhat, T.J.M.T.P. Performance and Emission characteristics of a CI Engine fuelled with diesel and TiO₂ nanoparticles as fuel additive. *Mater. Today Proc.* **2015**, *2*, 3728–3737. [[CrossRef](#)]
37. Devarajan, Y. Experimental evaluation of combustion, emission and performance of research diesel engine fuelled di-methyl- carbonate and biodiesel blends. *Atmos. Pollut. Res.* **2019**, *10*, 795–801. [[CrossRef](#)]
38. Saxena, V.; Kumar, N.; Saxena, V.K. Multi-objective optimization of modified nanofluid fuel blends at different TiO₂ nanoparticle concentration in diesel engine: Experimental assessment and modeling. *Appl. Energy* **2019**, *248*, 330–353. [[CrossRef](#)]
39. Prabu, A.; Anand, R.B. Emission control strategy by adding alumina and cerium oxide nano particle in biodiesel. *J. Energy Inst.* **2016**, *89*, 366–372. [[CrossRef](#)]
40. Hoseini, S.S.; Najafi, G.; Ghobadian, B.; Ebadi, M.T.; Mamat, R.; Yusaf, T. Biodiesels from three feedstock: The effect of graphene oxide (GO) nanoparticles diesel engine parameters fuelled with biodiesel. *Renew. Energy* **2020**, *145*, 190–201. [[CrossRef](#)]
41. Anand, R.; Kannan, G.; Nagarajan, S.; Velmathi, S. Performance emission and combustion characteristics of a diesel engine fueled with biodiesel produced from waste cooking oil. *SAE Tech. Pap.* **2010**. [[CrossRef](#)]
42. Pan, M.; Qian, W.; Zheng, Z.; Huang, R.; Zhou, X.; Huang, H.; Li, M. The potential of dimethyl carbonate (DMC) as an alternative fuel for compression ignition engines with different EGR rates. *Fuel* **2019**, *257*, 115920. [[CrossRef](#)]
43. Kalam, M.A.; Masjuki, H.H. Testing palm biodiesel and NPAA additives to control NO_x and CO while improving efficiency in diesel engines. *Bioenergy* **2008**, *32*, 1116–1122. [[CrossRef](#)]
44. Atmanli, A. Comparative analyses of diesel–waste oil biodiesel and propanol, n-butanol or 1-pentanol blends in a diesel engine. *Fuel* **2016**, *176*, 209–215. [[CrossRef](#)]
45. Konishi, T.; Klaus, E.E.; Duda, J.L. Wear Characteristics of Aluminum-Silicon Alloy under Lubricated Sliding Conditions. *Tribol. Trans.* **1996**, *39*, 811–818. [[CrossRef](#)]
46. Habibullah, M.; Masjuki, H.H.; Kalam, M.A.; Zulkifli, N.W.M.; Masum, B.M.; Arslan, A.; Gulzar, M. Friction and wear characteristics of Calophyllum inophyllum biodiesel. *Ind. Crop. Prod.* **2015**, *76*, 188–197. [[CrossRef](#)]

